Theoretical and Applied Climatology
https://doi.org/10.1007/s00704-022-04274-3

ORIGINAL PAPER

Machine learning-based downscaling: application of multi-gene genetic programming for downscaling daily temperature at Dogonbadan, Iran, under CMIP6 scenarios

Majid Niazkar[1] · Mohammad Reza Goodarzi[2] · Atiyeh Fatehifar[2] · Mohammad Javad Abedi[3]

Received: 30 November 2021 / Accepted: 30 October 2022

Abstract
In this study, two machine learning (ML) models, named multi-gene genetic programming (MGGP) and artificial neural network (ANN) are used to downscale outputs of three general circulation models using CMIP6. According to the literature, it is the first time that MGGP has been used for downscaling purposes. The historical measurements of daily temperature observed at Dogonbadan station, Kohgiluyeh and Boyer-Ahmad Province, Iran, were divided into training (1985–2006) and test (2006–2015) parts. The results indicate that MGGP performed slightly better than ANN in terms of three criteria considered for the test data. The ML-based downscaling models were also used for forecasting daily temperature for 30 years (2030–2060) in the future for two scenarios (SPP1 and SPP5). The results of the Mann–Kendall's test and Sen's slope estimator for estimating temperatures in future overall indicate an increasing trend compared to the observed data. The future estimations demonstrate that the significant increase of the minimum daily temperature may yield cooler summers, whereas the small reduction of the maximum daily temperature may result in warmer winters in the future in the study area under investigation. Finally, pros and cons of MGGP as a downscaling model were presented for further applications in impact assessments of climate change.

1 Introduction

Study of climate change effects is one of the important topics in the field of water resources. In essence, many investigations have been conducted in light of impact assessment of climate change. The Intergovernmental Panel on Climate Change (IPCC) estimates global warming at around 1.58 °C in the special report (IPCC 2018). Atmospheric warming and continuous emission of greenhouse gases cause heating of all components of the climate system. The increase in temperature also brings about many changes in precipitation patterns on a local to regional scale. Furthermore, these changes have led to an increase in extreme events, such as floods and droughts (Mendez et al. 2020; Goodarzi et al. 2020, 2022). In this context, climate models are accounted as a useful tool for detecting past and future climate changes, while the results of these models have been widely used. The first phase of CMIP began 20 years ago under the auspices of the World Climate Research Program Working Group on Paired Models. The CMIP, which is now in its sixth phase, helped to develop and evaluate models that increasingly provide comprehensive representations of the climate system (Eyring et al. 2016). In this regard, phase 6 was developed by integrating the common socio-economic trajectories alongside the trajectories representing greenhouse gas concentrations to analyze feedback between climate change and socioeconomic factors, such as global population growth, economic development, and technological advances (Riahi et al. 2017). Shared socioeconomic pathway (SSP) covers a different number of economic and social areas (Gidden et al. 2019a, b). Basically, the sixth report covers

✉ Mohammad Reza Goodarzi
Goodarzimr@yazd.ac.ir

Majid Niazkar
majid.niazkar@unimi.it

Mohammad Javad Abedi
mgabedi13@yahoo.com

[1] Department of Agricultural and Environmental Sciences, University of Milan, Via Celoria 2, 20133 Milan, Italy

[2] Department of Civil Engineering, Yazd University, Yazd, Iran

[3] Department of Civil Engineering, Water Resources Management Engineering, Yazd University, Yazd, Iran

Published online: 11 November 2022

a wide range of updated models of the fifth report and new SSP scenarios. The importance of hydroclimatic variations on regional and global water cycles led to a wide range of research studies to explore temperature and precipitation changes, particularly in the future.

Hao et al. (2013) evaluated the monthly temperature and precipitation of the continents of Asia, Africa, and South America using 13 models of the fifth report. Their results demonstrated that these models were closely correlated with observational data (Hao et al. 2013). Akurut et al. (2014) examined effects of climate change on Lake Victoria rainfalls in East Africa in the twenty-first century using the outputs of the fifth report models under two scenarios (RCP4.5 and RCP8.5) in the period of 2075–2040 (Akurut et al. 2014). In a more recent study, Almazroui et al. (2020) analyzed changes in temperature and rainfall in six south Asian countries during the twentieth century using the output of the sixth report. They predicted that pre-temperature increased by more than 6 °C under the SSP5-8.5 scenario in the south Asia. The projected winter rainfall also showed a significant increase in the western Himalayas and a decrease in the eastern Himalayas. On the other hand, they reported a large increase of summer rainfall in most parts of the south Asia (Almazroui et al. 2020). Also, Yue et al. (2021) examined future climate changes of the Yangtze River Basin in China based on the CMIP6 models under three new scenarios (SSP1-2.6, SSP2-4.5, and SSP5-8.5). The increase of temperature and precipitation under the SSP5-8.5 scenario was more than that of other scenarios (Yue et al. 2021).

A noteworthy point in using these models is the need to downscale outputs of general circulation models (GCMs), which utilize physically based equations for estimating the response of the global climate system to global warming (Nourani et al. 2019). Basically, the downscaling process is divided into two approaches: (a) statistical and (b) dynamical downscaling. The former primarily aims to develop predictand-predictor relationships using observed climatic variables and GCM outputs, while the latter extracts information by exploiting GCM outputs as boundary conditions of regional climate models (Wood et al. 2004; Nourani et al. 2019).

According to the literature, extensive studies have been conducted on the capability of linear and nonlinear regressions in the statistical downscaling of climatic variables. These investigations utilized different techniques including multi linear regression (MLR) (Sachindra et al. 2014), generalized linear models (GLMs) (Beecham et al. 2014), artificial neural networks (ANNs) (Tripathi et al. 2006; Ahmed et al. 2015; Nourani et al. 2019), support vector machine (SVM) (Sachindra et al. 2013; Goly et al. 2014), relevance vector machine (RVM) (Ghosh and Mujumdar, 2008; Okkan and Inan, 2015), genetic programming (GP) (Coulibaly 2004; Sachindra et al., 2018a, b), and gene expression programming (Hashmi et al., 2011; Sachindra et al. 2016). For instance, Chen et al. (2012) evaluated two methods, SVM and statistical downscaling model (SDSM), on a daily downscale of precipitation in the Hanjiang catchment, which is located in the north western China with an annual rainfall of 900 mm and an average temperature of 12–16 °C. Furthermore, they compared the output of two GCMs (HadCM3 and CGCM3). The results indicated that the performance of SVM for rainfall simulation is better than that of SDSM (Chen et al. 2012). Duan and Mei (2014) compared three statistical downscaling methods (SVM, SDSM, and LARS-WG) in simulating daily rainfall in different climates of China. To be more specific, they used observational data from 31 stations across China. Their results showed that each of these methods has a certain accuracy and efficiency appropriate to the type of climate. However, the general performance of SDSM was found to be the highest for most stations (Duan and Mei 2014). Vu et al. (2016) conducted a study with the aim of downscaling of the output of the ECHAM5 model using ANN to simulate and predict seasonal precipitation at the Bangkok rain gauge station in Thailand. Their study revealed that there is a high correlation between observational and simulated values, while ANN showed a high accuracy for downscaling purposes (Vu et al. 2016).

Based on the literature, GP, as a powerful machine learning (ML) method, has been applied for statistical downscaling in several studies. Generally, GP-based models obtained approximately 10% smaller root mean square error (RMSE) compared to linear regression (e.gCoulibaly 2004; Hashmi et al. 2011). Among the earliest studies that employ GP for building downscaling models, Coulibaly (2004) reported that GP performed better than MLR for downscaling both daily minimum and maximum temperature. Furthermore, Sachindra et al. (2018a) applied four ML methods (GP, ANN, SVM, and RVM) for statistical downscaling of monthly precipitation across the Australian State of Victoria for 1950–2014. According to the results, RVM and ANN are suggested for downscaling high extremes of precipitation for flood prediction studies, whereas RVM is recommended for downscaling low extremes of precipitation for drought analysis investigations. Moreover, Zerenner et al. (2018) proposed multi-objective genetic programming not only for minimizing RMSE but also for generating the probability distribution of the predictand. As a result, they obtained a set of Pareto optimal solutions for deterministic and stochastic downscaling of daily precipitation. In addition, Sachindra et al. (2018b) assessed how effective GP performs in selecting a combination of optimum GCM variables for downscaling purposes. Since GP is capable of developing a predictor-predictand relationship without the need for selecting predictors in advance, it may be used for such a purpose. Also, Sachindra et al. (2019) discussed advantages and disadvantages of GP combined with wavelet transform for a

downscaling exercise. They compared GP and GLM with and without considering wavelet transform for precipitation downscaling at 50 stations located in the state of Victoria in Australia in the periods of 1950–2014. The results show that when GP is combined with wavelet analysis, unphysically large values of local-scale weather data are considered significantly in the simulation, which may yield an inevitable increase of downscaling errors (Sachindra et al. 2019). Furthermore, Sachindra and Kanae (2019) suggested that parallel multi-population genetic programming can be a better downscaling tool than the traditional GP because it has not only better generalization skills but also practically generated fewer unphysically large outliers. More recently, Kumar et al. (2021) investigated wavelet-based hybrid models (wavelet transform-based feed-forward neural network (WT-FF-NN) and wavelet transform-based nonlinear auto regressive with exogenous inputs Network (WT-NARX-NN)) for downscaling of daily precipitation of the Krishna River basin, in the Indian subcontinent. The results of the wavelet-based hybrid methods were compared with those of four ML methods (MLR, SDSM, GP, and ANN). It was demonstrated that WT-FF-NN and WT-NARX-NN performed better in capturing the regional precipitation patterns and extreme events. Additionally, Zerenner et al. (2021) introduced a multi-objective optimization problem, whose conflicting objective functions are minimizing the RMSE and increasing the consistency in the distribution between the model and observations. They developed deterministic and stochastics multi-objective GP-based downscaling models, while GLMs were set as a benchmark. It was indicated that no unique model outperforms others. To be more specific, although the deterministic downscaling models with low RMSE achieved better results than the respective stochastic models, the stochastic models with low integrated quadratic distance yielded a slight improvement in comparison with the respective deterministic models for most cases.

In most of the studies conducted with the sixth report, dynamic downscaling has been used. Additionally, since SDSM and LARS-WG models were inconsistent with CMIP6, the scenarios of report 5 have been already applied in most of statistical downscaling studies. However, the use of other statistical methods, such as change factor, with the sixth report is common.

In this study, the main purpose is to develop ML-based downscaling models considering the sixth report. CMIP6 models have recently been considered because of the new generation of climate models and their new start year (2015 for CMIP6 vs. 2006 for CMIP5) for future scenarios as well as a new set of specifications for concentration, emission, and land use scenarios (Gidden et al. 2019a, b). In this study, performances of ANN and a modified version of GP, called multi-gene genetic programming (MGGP), are assessed. Based on the literature review, this is the first time that MGGP has been applied as a statistical downscaling tool for developing predictand-predictor relationships. Since MGGP is capable of capturing complex trends, it is postulated that this application increases the precision of downscaling models.

2 Materials and methods

2.1 Study area

Gachsaran city is located in Kohgiluyeh and Boyer-Ahmad Province, Iran, and has a tropical winter. The eastern and tropical-arid in the western half of Dogonbadan region has pastures, forests, and vast agricultural lands, and consequently, it is very important to pay attention to water management issues in this part of the province. Figure 1 depicts the location of the area.

As shown, Dogonbadan station located in Gachsaran city has a longitude of 50 degrees and 78 min east and latitude of 30 degrees 36 min north and is 750 m above sea level. The average minimum temperature in this region is 3 to 4 degrees below 0 in January and February, respectively, while the maximum temperature is up to 50 degrees Celsius in July and August. The average annual rainfall between 1985 and 2014 was 364.5 mm, which fluctuated between 132.5 to about 527 mm in different years.

The 30-year historical measurements of daily temperature at Dogonbadan station were collected in this research. This database was divided into two parts: (a) training data (from 1985 to 2006) and (b) test data (from 2006 to 2015). The former was used for training ML-based downscaling methods, while the latter was utilized for testing their performances. For a better visualization, Fig. 2 illustrates both parts of the observed temperature data. As shown, a small number of data, particularly during 1992–1993 and in 2010, was not measured at the station in question and, therefore, they were excluded from the simulation in this study. By excluding the missing data, the total number of data becomes 10,333 (7316 for training and 3017 for test data). Thus, since the dataset has a large number of observed data so that there is enough data for training ML-based models, excluding the date of missing data from the dataset does not hinder the performance of the simulation process.

2.2 Selected climatic models CMIP6

To evaluate the trend of temperature variations in the selected station, three GCM models in accordance with the sixth IPCC report were used. In the climate models of the sixth phase, the combination of common socio-economic trajectories along with the trajectories representing the concentration of greenhouse gases was used to analyze the feedback between climate change and socio-economic factors,

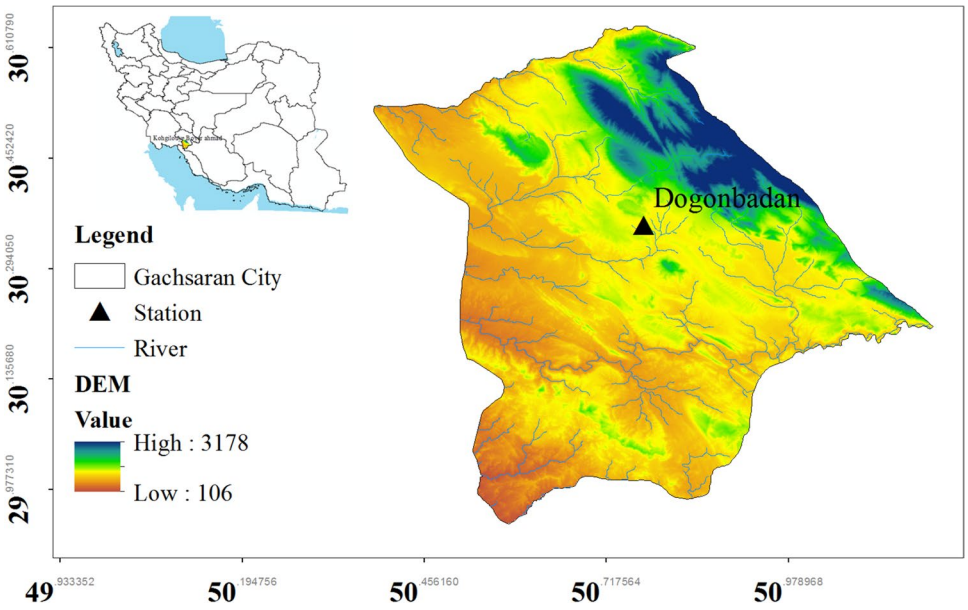

Fig. 1 Location of the study area

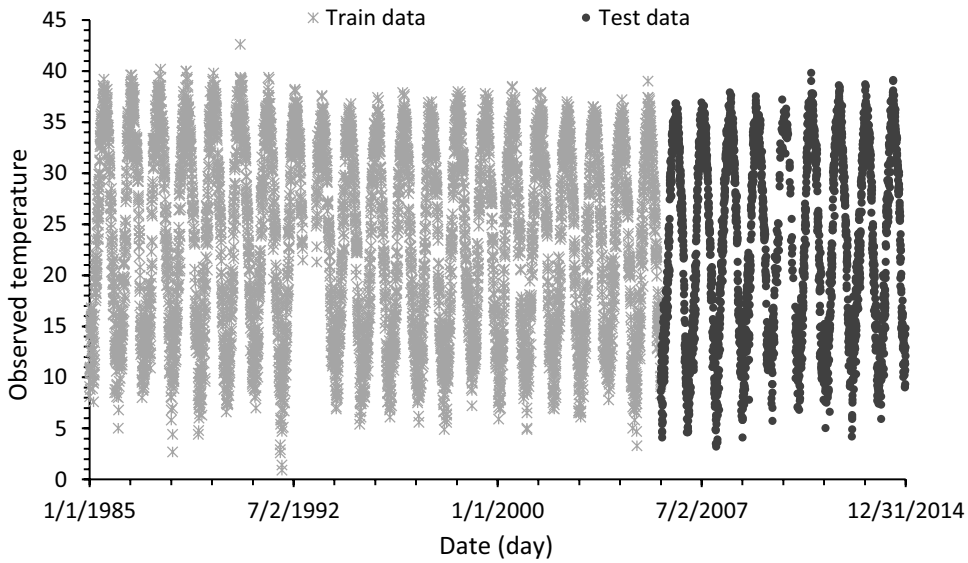

Fig. 2 Observed temperature of the training and test data

such as global population growth, economic development, and technological advances (Riahi et al. 2017). The output of the sixth report models is under the new SSP scenarios, which provide trajectories of common socio-economic sectors and different concentrations of greenhouse gas (RCP) emissions. The scenarios of the sixth report, which include 5 main subgroups, include quantitative indicators (population, urbanization, regional and trans-regional economic development, etc.) and emphasize on generalized scenarios (effects, adaptation, and reduction of vulnerability), energy program, and land use change, etc.

Three climatic models, named CanESM5, BCC-CSM2-MR, and MRI-ESM2-0, were utilized in this study. They are adopted from the set of available CMIP6 models with optimistic scenario SSP1-2.6 (synchronized with scenario RCP2.6 from the series of models CMIP5) and pessimistic scenario SSP5.8.5 (synchronized with scenario RCP8 5). CMIP5 model series was used. The two 30-year periods were selected in this study. The two periods entail the historical period of 1985–2015 and the future period of 2030–2060. Information was downloaded from the ESGF climate site (https://esgf-node.llnl.gov/search/cmip6/). Table 1 summarizes the descriptions of the models used.

The first climatic model from the sixth phase set, i.e., CanESM5 model, which was released in 2019, is essentially an updated CanESM2 model in the fifth report by the Canadian Center for Climate Modeling and Analysis. This update includes improvements in the atmosphere, land surface, and terrestrial ecosystem models. Major modifications to

Table 1 CMIP6 GCMs selected

GCM	Host Institute	Experiment	Resolution	Variant	References
CanESM5	Canadian Centre for Climate Modelling and Analysis,	Hist SSP1-2.6 SSP5-8.5	500	r1i1p1	Swart Neil et al. (2019)
BCC-CSM2-MR	Beijing Climate Center, China Meteorological Administration, China	Hist SSP1-2.6 SSP5-8.5	100	r1i1p1	Wu et al. (2018; 2019)
MRI-ESM2-0	Meteorological Research Institute (MRI), Japan	Hist SSP1-2.6 SSP5-8.5	100	r1i1p1	Yukimoto et al. (2019)

CanESM2 are the implementation of completely new models for ocean, sea ice, and marine ecosystems. The horizontal separation in the atmosphere and land is 500 km and in the ocean and sea is 100 km (Swart Neil et al., 2019).

The second climatic model is the Beijing Climate Model is the CSM2-MR version of the sixth phase model suite and the updated version in the fifth report. It requires more processing time (up to 50%) than the fifth BCC-CSM1.1 m report version. The new version was released in 2017 with a resolution of 100 km in the atmosphere and land and 50 km in the ocean and sea (Wu et al. 2018). The historical period of this model is from 1850 to 2014. One of the most important features of this model compared to previous ones can be summarized in the following: (1) better simulation of energy budget in the upper atmosphere, (2) improved precipitation and GCM design in the world and East Asia, and (3) better simulation of climate change in different time periods such as trends Noted global warming (Wu et al. 2019).

Finally, the MRI-ESM2-0 model is one of the climatic models of the Japan Meteorological Research Institute (MRI), which is based on the previous models, MRI-CGCM3 and MRI-ESM1, which were in CMIP5. The errors of the new version are much less than the previous ones, while the horizontal separation of this model is 250 km for suspended particles and chemistry of atmosphere and 100 km for atmosphere land and ocean. In this model, various improvements have been made to the new scheme for clouds, which has led to a significant reduction in short- and long-wavelength errors as well as net radiation above the atmosphere. Overall, the MRI-ESM2-0 model represents a more realistic reproduction of the climate average and annual variability (Yukimoto et al. 2019). Finally, the validity coefficients of the GCM models for temperature before downscaling are presented in Table 2.

Table 2 Validity coefficients of GCM models

Models	NSE	R^2
CanESM5	0.76	0.77
MRI-ESM2-0	0.97	0.98
BCC-CSM2-MR	0.88	0.96

Generally, scenarios are an important complement to predicting GCM models. These scenarios are designed to address a wide range of future societal and economic challenges in adapting to or mitigating climate change. These scenarios allow for an organized exploration of the challenges associated with adaptation policies and possible future adjustments (Riahi et al. 2017). In summary, the scenarios are divided into five subgroups:

(1) SSP1: Taking a green and sustainable path (challenges to low compatibility)—global commonalities and nature and environmental constraints are respected. Focus more on people than on economic development. SSP1 assumptions include sustainable consumption, low population growth, increased energy efficiency, faster replacement of renewable energy, and greater global cooperation. The next two numbers in the SSP126 standard scenario (SSP1-2.6) indicate the radiation induction obtained by 2100 in this scenario. Forcing this scenario with W/m^2 2.6, which is a reconstruction of the optimistic RCP2.6 scenario in the fifth report.

(2) SSP2: Medium (medium challenges)—there is some cooperation between governments, but it is difficult to expand. Global population growth is moderate. Global and national institutions are moving towards achieving the goals of sustainable development but are not making slow progress. Environmental systems are deteriorating, although there have been some improvements, and overall resource and energy intensity is declining. In general, the assumptions represent the intermediate conditions; under these conditions, socio-economic development is in line with normal conditions.

(3) SSP3: Regional competition (major challenges to adjustment)—revived nationalism raises concerns about competitiveness and security and regional conflicts in countries that increasingly focus on domestic or regional issues. Countries focus on achieving energy and food security goals in their regions at the expense of extensive development. Some areas suffer

from severe environmental damage due to low international priorities for addressing environmental concerns. It envisions a world with many challenges to adjustment-related policies, including high population growth that leads to high food and energy demand and regional competition; such conditions hinder social and technological development. SSP370 radiation emission equal to 7 W/m^2 by 2100, the distance between RCP6 and RCP8.5.

(4) SSP4: Inequality (low challenges to reduce, large challenges to adaptation)—reflects a highly unequal world with inequality in economic and political power, leading to rising inequality at home and abroad throughout the twenty-first century. Conflict and unrest are also expected to increase. Also, the development of advanced technology in various sectors is great and the energy system will be diverse. SSP245 complies with RCP4.5 with a radiant induction of 4.5 W/m^2 by 2100.

(5) SSP5: Development of fossil fuels (big challenges to reduce, low challenges to adaptation)—increasingly competitive global markets lead to innovation and technological advancement. But socio-economic development is based on the intense exploitation of fossil fuel resources with a high percentage of coal and a high-energy lifestyle around the world. In short, this scenario represents an advanced yet fossil fuel world in which energetic lifestyles are used. The radiant induction of the SSP585 standard scenario (SSP5-8.5) is 8.5 watts per square meter (W/m^2), which is consistent with the RCP8.5 scenario in the sixth report and combined with socio-economic conditions (Riahi et al. 2017; O ' Neill et al. 2017; Estoque et al. 2020).

According to the IPCC Regional and Atlas Global Information (https://interactive-atlas.ipcc.ch/), and based on the sixth report in the evaluation of 34 GCM models, Iran will experience a global average temperature change of 1.5 degrees under two scenarios SSP1-2.6 and SSP5-8.5 and its temperature has increased by 1 °C. Figure 3 shows the global atlas for these two scenarios.

2.3 Downscaling models

In this study, two ML methods were used to downscale GCM outputs. These ML methods are summarized in the following:

2.3.1 Artificial neural network

ANN has been widely used as an estimation tool in numerous fields of research. In the parlance of ML methods, it takes advantage of a multi-layer network to develop a suitable relationship that can describe physical behavior of a complicated system. In essence, a typical network in ANN has three main kinds of layers, called input, hidden, and output layers, whose neurons are merely responsible to take data and transfer it to the neurons of the adjacent layer. Basically, the back-and-forth data flow within an ANN structure enables it to capture a relation between input and output variables. As an ML method, ANN can tackle various problems regardless of any requirement about the physical background of the data involved. Finally, ANN features turn it into an adequate ML method in the field of water resources.

In this study, a three-layer ANN model with feed-forward back-propagation and the Levenberg Marquardt optimization algorithm was utilized to downscale GCM outputs. The controlling parameters of ANN were considered the same as those implemented in previous studies (Niazkar 2020). Additionally, the ANN architecture consists of three, ten, and one neurons in the input, hidden, and output layers, respectively. The input data, which was given to the input layer, are normalized GCM outputs, while the dimensionless daily temperature was set as the output variable. Furthermore, the training data depicted in Fig. 2 was used to train ANN. The performance of the trained ANN model was tested using the test data shown in Fig. 2. The ANN-based downscaling model that performs acceptable for both training and test data was deployed to forecast daily temperature in future.

2.3.2 Multi-gene genetic programming

GP was fundamentally designed to facilitate the well-documented genetic algorithm (GA) with an estimation capability. To be more precise, GP, as a ML method, exploits not only GA as a remarkable optimization engine but also a flexible configuration to determine an estimation model. These features make a powerful prediction model out of GP, which does not require prior information about the shape of the prediction model in question. MGGP is one of improved variants of GP, whose essential steps follow those assumed in GA. Although both MGGP and GP utilize a tree-like structure, MGGP, unlike GP, can contain more than one gene (tree) in each individual (relation). As a result, the MGGP solution is a combination of one or more genes, whose equations are first weighted and then summed up. In other words, the algebraic summation of the weighted equations associated with genes becomes the MGGP-based model. Calculating weighting coefficients is a part of MGGP, which makes it different from the classical GP version. In addition, a bias is commonly added to the summation in MGGP. Finally, considering more than one gene in each individual makes MGGP more flexible so that it can be used to delineate complicated relationships available between input and output vectors.

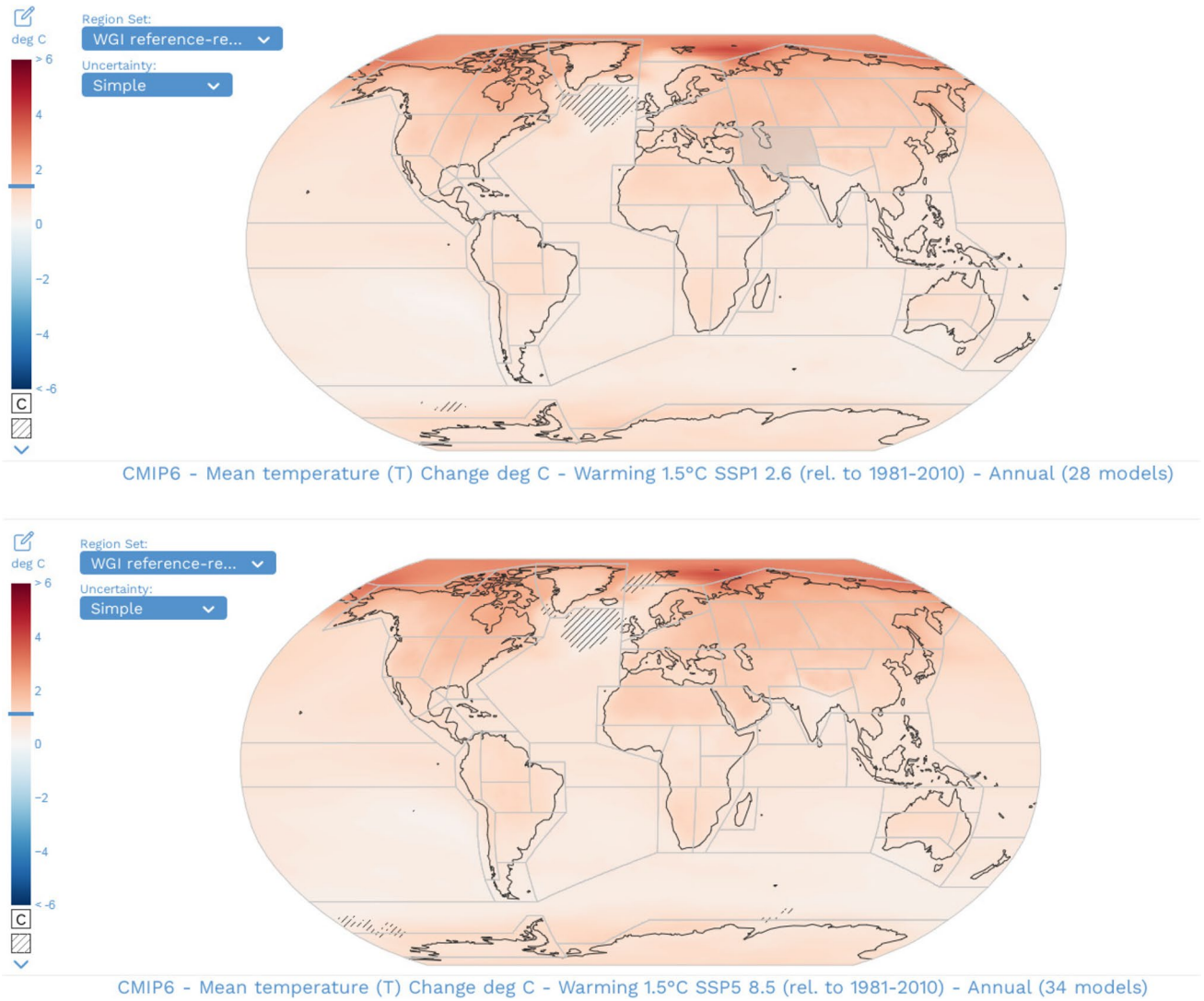

Fig. 3 Atlas of temperature changes under 1.5 °C temperature rise

In this study, GPTIPS, which is an open-access MATLAB code of MGGP (Searson 2009), was used to develop MGGP-based downscaling models. This MGGP version has been already applied to other water resources applications in the literature (Niazkar and Zakwan 2021; Zakwan and Niazkar 2021, 2022). In GPTIPS, MGGP attempts to minimize RMSE as an objective function and solves the optimization problem using GA. The RMSE indicates the error computed between the estimated and observed normalized daily temperature in this study. Since the nature of MGGP, and even GP, relies on solving an optimization problem, each run of MGGP may yield a distinct solution. Hence, in this study, GPTIPS was run for more than 50 times to ensure that a reliable MGGP-based model was obtained. The number of MGGP runs (i.e., 50) was adopted from the literature (Lee and Suh 2020; Niazkar and Zakwan 2021). Furthermore, Table 3 lists the MGGP controlling parameters used in this study. The selected values were also adopted from previous studies in the literature (Niazkar and Zakwan 2021). According to Table 3, different functions implemented in GPTIPS were set as admissible functions to be used in the MGGP-based estimation model, while MGGP does not require to know which types of equations a prediction model consists of in advance. In the process of MGGP, normalized GCM outputs were used as the input variables, while the dimensionless daily temperature was the output in GPTIPS. The performance of each one of 50 MGGP-based models was tested for both training and test data, while the one with the lowest RMSE was reported as the best-fitted MGGP downscaling model.

2.4 Trend analysis

In this study, two common trend analysis methods were used to check whether the observed and estimated temperatures have any trend. These methods are presented concisely as follows.

Table 3 MGGP controlling parameters

Parameter	Values
Function set	Four basic mathematical operations, trigonometric function, square function, exponential function and operations
Number of generations	120
Stopping criterion	0.001
Maximum number of genes allowed in individual	5
Maximum tree depth	4
Crossover events	0.85
High-level crossover	0.2
Low-level crossover	0.8
Sub-tree mutation	0.9
Replacing input terminal with another random terminal	0.05
Gaussian perturbation of randomly selected constant	0.05
Direct reproduction	0.05
Ephemeral random constants	[− 10, 10]

2.4.1 Mann–Kendall test

The Mann–Kendall (MK) test is a non-parametric trend analysis test commonly used for identifying trends in hydrological and meteorological data series (Hirca et al., 2022). Two advantages of MK test entail the independence of a particular statistical distribution and low effectiveness of extreme values (Partal and Kahya 2006). The null hypothesis in MK indicates that a data series has random attributions with no trend whereas the hypothesis one demonstrates the existence of a trend in the data series (Zakwan and Niazkar 2021, 2022). In general, the MK test is categorized into computational and graphical groups, which are summarized in the following:

(a) Computational MK method: The standard test statistic Z is calculated using Eq. 1 (Salmi et al., 2002):

$$Z = \begin{cases} \frac{S-1}{\sqrt{var(S)}} & if \quad s > 0 \\ 0 & if \quad s = 0 \\ \frac{S+1}{\sqrt{var(S)}} & if \quad s < 0 \end{cases} . \tag{1}$$

where $s = \sum_{i=1}^{n-1} \sum_{j=i+1}^{n} sgn(x_j - x_i)$, $var(S) = \frac{n(n-1)(2n+5) - \sum_{i=1}^{n} t_i(t_i-1)(2t_i+5)}{18}$, X_i and X_j are two ordered data subsets of data,

$$sgn(x_j - x_i) = \begin{cases} +1 & if \quad (x_j - x_i) > 0 \\ 0 & if \quad (x_j - x_i) = 0 \\ -1 & if \quad (x_j - x_i) < 0 \end{cases}, \text{ and } n \text{ is the sample size.}$$

According to the definition of Z, if the value of Z is either greater than + 1.96 or less than − 1.96, the data has a trend, which means that the null hypothesis is rejected. Otherwise, the data is trendless, and the null hypothesis is confirmed.

(b) Graphic MK method: This is a 5% confidence-level test, while interpretations of this method rely on the graphs obtained from the statistical values of $U(t_i)$ and $\overleftarrow{U}(t_i)$. In this study, the graphic MK test was used as a sequence according to Sneyers' (1990) study, in which the statistical values of $U(t_i)$ and $\overleftarrow{U}(t_i)$ were calculated as follows: (1) First, the data is sorted by year ranking (y_i). (2) The smaller rank (t_i), which is the number of the data (n_i) before the data under consideration (y_i) that are smaller than y_i, is computed. (3) Finally, $U(t_i)$ is determined by Eq. 2:

$$U(t_i) = \frac{\left[t_i - E(t_i)\right]}{\sqrt{var(t_i)}} \tag{2}$$

where $E(t_i) = \frac{i(i-1)}{4}$ and $var(t_i) = \frac{[i(i-1)(2i+5)]}{72}$ are the mean and variance of $t_i = \sum_{k=1}^{i} n_k$, respectively.

$\overleftarrow{U}(t_i)$ is calculated similar to the method utilized for computing $U(t_i)$. To be more specific, the data for calculating $U(t_i)$ and $\overleftarrow{U}(t_i)$ are sorted and ranked according to the occurrence year, while the year of occurrence in $U(t_i)$ and $\overleftarrow{U}(t_i)$ is in ascending and descending orders, respectively.

After computing and plotting $U(t_i)$ and $\overleftarrow{U}(t_i)$, the trend analysis can be conducted based on these two graphs. At the starting point, these two graphs will intersect. Furthermore, if $|U| > 1.96$, which indicates that the $U(t_i)$ graph crosses the two lines $Y = 1.96$ and $Y = -1.96$, the trend in the series in question can be considered meaningful. If $U > 0$ or the $U(t_i)$ graph overall has an increasing trend, a significant

upward trend is reported. If $U<0$, the trend is significant and decreasing. Moreover, if the $U(t_i)$ and $U\ (t_i)$ graphs intersect in the range of − 1.96 and 1.96, it denotes a sudden change in the mean value.

2.4.2 Sen's slope estimator

Sen's slope estimator is a nonparametric test commonly used to identify trends in a series as well as indicating the magnitude of the trend. In essence, this trend analysis method is based on calculating a median slope for the time series under the investigation and judging the significance of the slope obtained at different levels of confidence. Estimating the Sen's slope requires a time series consisting of at least 10 values. Similar to the MK method, it utilizes the analysis of differences between observations of a time series. Additionally, it can also be easily used when there is missing data (Serrano et al. 1999). Finally, the general steps of this test are as follows:

A) Calculate the slope between each pair of observational data using Eq. 3:

$$Q = \frac{X_t - X_s}{t - s} \tag{3}$$

where X_t and X_s are the observed data at times t and s, respectively, and t is a time unit after time s. By applying this relation to both pairs of the observed data, a time series of calculated slopes is obtained. To be more specific, it is determined by calculating the middle of this time series of trend line slope ((Q)). A positive value of (Q) indicates an uptrend, while a negative value denotes a downward trend.

B) Calculate (c_α) at the confidence levels tested using Eq. 4:

$$c_\alpha = Z_{1-\alpha/2} \times \sqrt{var(s)} \tag{4}$$

where Z is the standard normal distribution statistic, which can take different values in a two-domain test depending on the confidence levels considered. To be more precise, c_α for 95% and 99% confidence levels is equal to $Z = 1.96$ and $Z = 2.58$, respectively (Salmi et al., 2002).

2.5 Sensitivity analysis

Basically, sensitivity analysis (SA) delineates how much an independent variable impacts on the results of an ML-based statistical downscaling method. For this purpose, the SA percentage of the temperature predicted by a downscaling model in respect with each climate model was calculated using Eq. 5 (Zakwan and Niazkar 2021, 2022):

$$SA_i = \frac{T_{max}(x_i) - T_{min}(x_i)}{\sum_{i=1}^{N}\left[T_{max}(x_i) - T_{min}(x_i)\right]} \times 100 \tag{5}$$

where $T_{\max}(x_i)$ and $T_{\min}(x_i)$ are the minimum and maximum temperature. The former and latter parameter is computed by taking into account a typical GCM output (x_i) when average values of climatic models are substituted instead of the corresponding GCM outputs. According to Eq. 3, a higher value of the SA percentage indicates that the downscaling model is more sensitive to a specific variable.

2.6 Performance evaluation criteria

The performances of ML-based downscaling models were compared based on several criteria. These metrics are (1) RMSE, (2) Nash–Sutcliffe efficiency (NSE), (3) mean absolute error (MAE), (4) mean absolute relative error (MARE), (5) maximum absolute relative error (MXARE), and (6) determination coefficient (R^2). These criteria are presented in Eq. 6 to Eq. 11 (Niazkar 2021):

$$\mathrm{RMSE} = \sqrt{\frac{\sum_{i=1}^{\mathrm{N}}(\mathrm{T}_{\mathrm{obs}_i} - \mathrm{T}_{\mathrm{est}_i})^2}{\mathrm{N}}} \tag{6}$$

$$\mathrm{NSE} = 1 - \frac{\sum_{i=1}^{\mathrm{N}}(\mathrm{T}_{\mathrm{obs}_i} - \mathrm{T}_{\mathrm{est}_i})^2}{\sum_{i=1}^{\mathrm{N}}(\mathrm{T}_{\mathrm{est}_i} - \frac{\sum_{i=1}^{\mathrm{N}}\mathrm{T}_{\mathrm{obs}_i}}{N})^2} \tag{7}$$

$$\mathrm{MAE} = \frac{1}{N}\sum_{i=1}^{N}\left|\mathrm{T}_{\mathrm{obs}_i} - \mathrm{T}_{\mathrm{est}_i}\right| \tag{8}$$

$$\mathrm{MARE} = \frac{1}{N}\sum_{i=1}^{N}\left|\frac{\mathrm{T}_{\mathrm{obs}_i} - \mathrm{T}_{\mathrm{est}_i}}{\mathrm{T}_{\mathrm{obs}_i}}\right| \tag{9}$$

$$\mathrm{MXARE} = \max\left(\frac{\mathrm{T}_{\mathrm{obs}_i} - \mathrm{T}_{\mathrm{est}_i}}{\mathrm{T}_{\mathrm{obs}_i}}\right)\mathrm{for\,i} = 1, \ldots, \mathrm{N} \tag{10}$$

$$R2 = \left\{\frac{\sum_{i=1}^{\mathrm{N}}[(\mathrm{T}_{\mathrm{obs}_i} - \frac{1}{N}\sum_{i=1}^{N}\mathrm{T}_{\mathrm{obs}_i})(\mathrm{T}_{\mathrm{est}_i} - \frac{1}{N}\sum_{i=1}^{N}\mathrm{T}_{\mathrm{est}_i})]}{\sqrt{\sum_{i=1}^{\mathrm{N}}[(\mathrm{T}_{\mathrm{obs}_i} - \frac{1}{N}\sum_{i=1}^{N}\mathrm{T}_{\mathrm{obs}_i})^2(\mathrm{T}_{\mathrm{est}_i} - \frac{1}{N}\sum_{i=1}^{N}\mathrm{T}_{\mathrm{est}_i})^2]}}\right\}^2 \tag{11}$$

where T_{obs} and T_{est} are the observed and estimated daily temperature, respectively, and N is the number of data points. Based on the definition presented for each metric, higher performance of a downscaling model is associated with a lower value of RMSE, NSE, MAE, MARE, and MXARE and a higher value of R^2.

3 Results and discussion

The trained ANN and MGGP models were used to estimate the test data. Unlike ANN, MGGP develops an explicit relation for downscaling GCM outputs. The best-fitted model developed by MGGP for downscaling daily temperature at Dogonbadan station is shown in Eq. 12:

$$\begin{aligned}\overline{T} &= 0.2511\sin\left(x_2+x_3\right)-0.01105\sin\left(13.62x_1-13.62x_2\right)\\ &+0.1586sin\left(x_1+x_2\right)\left(2x_1+x_2+x_3\right)-\frac{0.01521\left(3x_2-2.3\right)}{x_2+x_3}\\ &+0.04653\sin\left(2x_2\right)\left(x_2-5.216\right)\left(x_1-x_2\right)+0.02518\end{aligned} \tag{12}$$

where $\overline{T}$ is dimensionless daily temperature and x_i is normalized outputs of the ith GCM. The maximum and minimum values of each parameter were used to turn it to a normalized one. For instance, $\overline{T}=\frac{T-T_{\min}}{T_{\max}-T_{\min}}$ where $T_{\max}$ and $T_{\min}$ are the maximum and minimum values of the total data of daily temperature, respectively.

As shown in Eq. 12, the best MGGP model exploits sinus function to downscale daily temperature. The use of this periodic function for downscaling daily temperature conforms to the periodic variation of daily temperature, as presented in Fig. 2. Although this selection was achieved by running MGGP for more than 50 times, it emphasizes how promising can MGGP perform in determining a suitable function from a set of various functions.

Figure 4 depicts the estimated vs. observed daily temperature values for both training and test data. As shown, the number of data points is adequately enough so that an ML-based downscaling method can be trained with a suitable dataset. In addition, the sparsity of daily temperature measurements is considerable in the available data, which has a negative influence on the accuracy of the downscaling results. Obviously, the existing variations in daily temperature requires powerful nonlinear techniques to capture the trends available in the observed data.

Forecasting hydroclimatic variables incorporating climate change impacts is one of the benefits of applying downscaling models. This practice can provide a new outlook on how a particular hydroclimatic variable may vary in a certain period of time in the future. Such estimations may give decision-makers a wake-up call on the impact of climate change on the specific study area under investigation. In this study, both ML-based downscaling methods were used to forecast daily temperature from 2030 to 2060 at Dogonbadan station for two scenarios (SPP1 and SPP5). The predicted results are displayed in Fig. 5. As shown, ANN provides relatively higher values of daily temperature than MGGP during the summer in the 30-year period under consideration. Furthermore, comparing Fig. 5 with Fig. 2 indicates that (1) the maximum daily temperature during the hottest days of summer will reduce in the study area and (2) the minimum daily temperature during the coldest days of the winter may be significantly increased. The latter increase is up to 10 °C for a few years between 2030 and 2060. Therefore, the findings of this study revealed that the range of daily temperature of the future period will be reduced in comparison with the historical period. Based on Fig. 5, the considerable increase of the minimum daily temperature may yield cooler summers, whereas the small decrease of the maximum daily temperature may result in warmer winters.

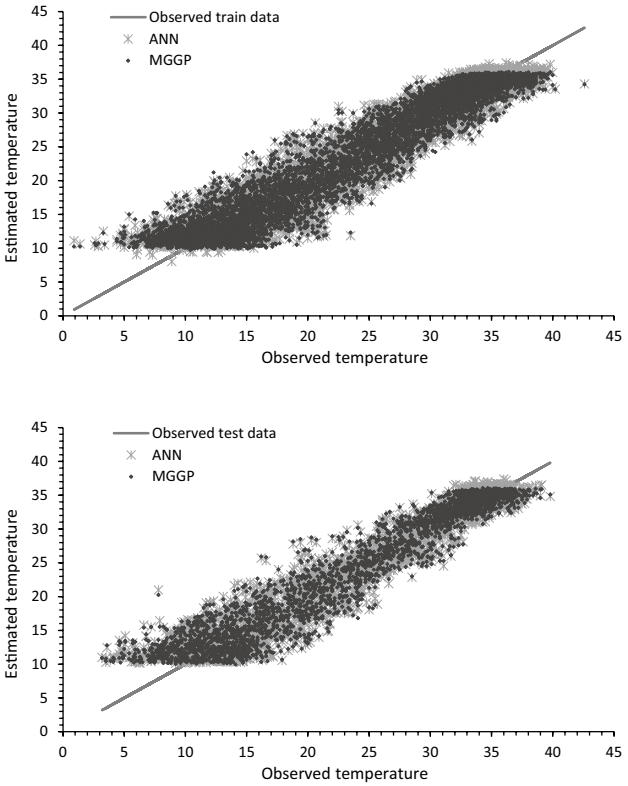

Fig. 4 Estimated temperature using ML-based statistical downscaling for the training and test data

3.1 Accuracy assessment of ML-based downscaling method

Figure 6 depicts values of different metrics to better investigate the performances of MGGP and ANN as statistical downscaling models. As shown, MGGP resulted in RMSE = 2.54, while ANN achieved RMSE = 2.50 for the training data. Therefore, ANN yielded 1.48% improvement in RMSE obtained by MGGP for the training data. Nevertheless, MGGP reach slightly better RMSE than ANN for the test data (0.16%). Likewise, Fig. 6 demonstrates that even though ANN performed slightly better (1.82%) than

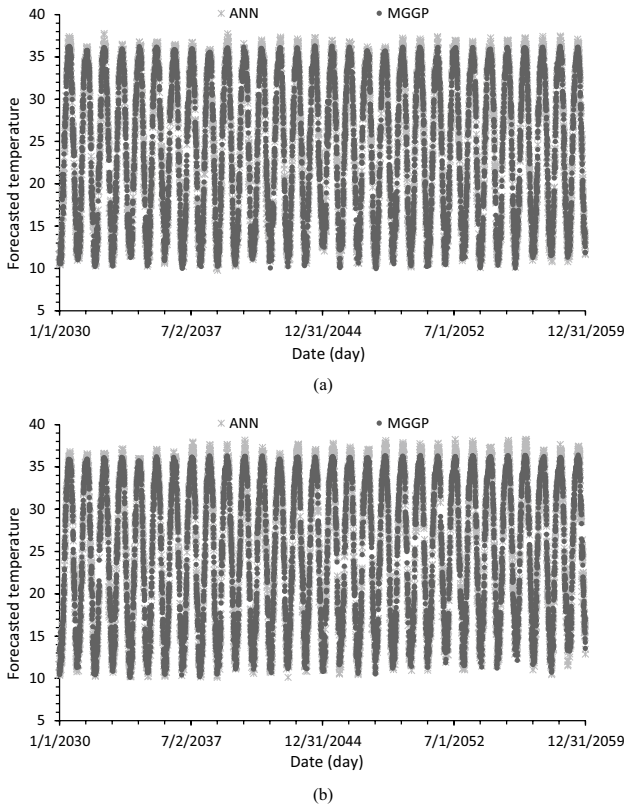

Fig. 5 Forecasted temperature using ML-based statistical downscaling for **a** SSP1 and **b** SSP5 scenarios

MGGP in respect with MAE for the training data, MGGP improved MAE of ANN by 0.62% for the test data. The performances of MGGP and ANN as ML-based downscaling models in terms of R^2 are the same as those for RMSE and MAE. Moreover, Fig. 6 shows that both MGGP and ANN achieved highly accurate values of MARE. According to Fig. 6, the best MXARE was obtained by MGGP for the training data, whereas ANN-based model reached the lowest MXARE for the test data. Overall, Fig. 6 indicates precise performances of ML-based downscaling models based on the criteria considered, while the best model may be different depending on metrics.

3.2 Results of trend analyses

The MK test statistics were calculated and the corresponding graphs are depicted in Fig. 7. The graphs are plotted on an annual time scale for the observed temperatures and the ones estimated from two SSP1 and SSP5 scenarios in the study station. Based on changes of $U(t_i)$ and $\hat{U}(t_i)$ components in the corresponding graphs, the trend analysis results of the average annual temperatures can be interpreted. According to Fig. 7a, the changes in the average annual temperatures observed in the studied station have been decreasing with a negative trend in the period of 2014–1997, while there is a sudden change in 1986 and 1989. Furthermore, based on Fig. 7b, a short-term upward trend for the average annual temperature can be imagined in the period of 2059–2057. In addition, in the years 2032, 2035, 2045, and 2048, sudden changes in the average annual temperature have occurred in Fig. 7b. Figure 7c shows a long-term upward trend in the period 2059–2042, while sudden changes in the average annual temperature are estimated in the years 2031, 2032, 2036, 2038, and 2039.

Table 4 presents the trend of monthly temperature changes for observed and estimated data. As shown, the results of both trend analysis methods indicate no trend for the observed temperatures only in July. Furthermore, the results of the MK test for the observed temperatures demonstrate a decreasing trend in August and October with 99% confidence and in November with 95% confidence. According to Table 4, the results of the MK test for the temperatures estimated for the SSP1 scenario show a relative increase trend in January, February, and April with 95% confidence and in May with 99% confidence, respectively. Moreover, Table 4 reveals that the MK test identified an upward trend in all months with 99% confidence except in July for the SSP5 scenario, while the results of both MK and Sen's slope tests indicate divergence for October, November, and December for this scenario. Additionally, no significant trend is detected in the observed data. However, in most months of the year for the SSP5 scenario, there is a significant upward trend with 99% confidence, which indicates an increase in the Sen's slope compared to the observed data.

The Sen's slope diagrams for the observed and estimated temperatures are illustrated in Fig. 8. As shown, there is a tendency to increase the temperature based on the trends achieved for the SSP1 and SSP5 scenarios as opposed to the observed temperatures. Finally, according to Figs. 7–8 and Table 4, it can be concluded that both Sen's slope estimator and the MK test generally reach a general trend of temperature changes for the region in question.

3.3 Results of sensitivity analysis

Although results of GP-based downscaling models may be influenced by large outliers available in predictands (Sachindra et al. 2019), GP and its modified versions, such as MGGP, can serve as a tool for conducting sensitivity analysis. To be more precise, MGGP can determine a suitable set of equations for developing a prediction model (Zakwan and Niazkar 2021, 2022). In this study, impacts of variations of GCM outputs on the daily temperature, which was the output of the ML-based downscaling models, were investigated using the proposed MGGP-based model. The results of the sensitivity analysis, which

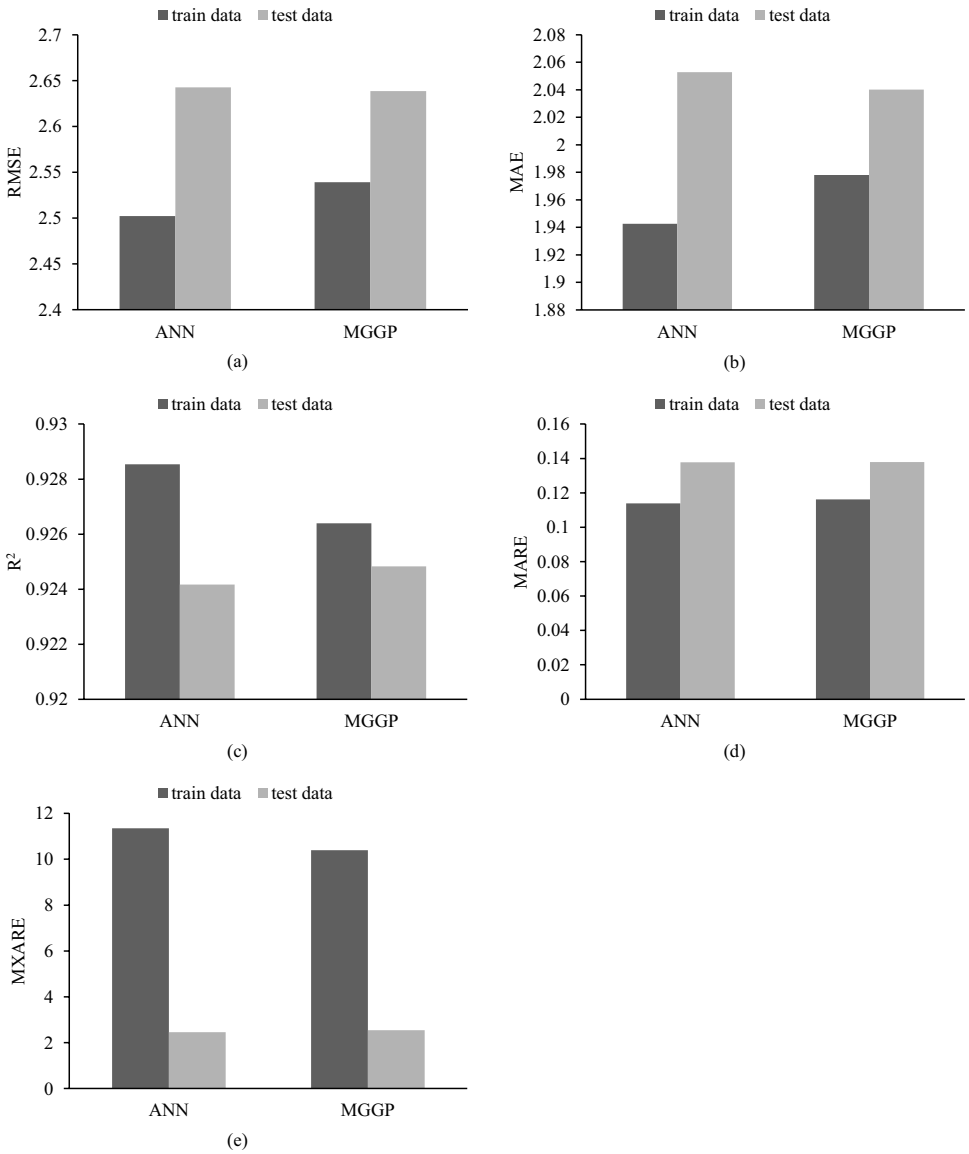

Fig. 6 Performance of ML-based statistical downscaling for estimating temperature for the training and test data: **a** RMSE, **b** MAE, **c** R^2, **d** MARE, and **e** MXARE

provides an appropriate perspective on which climatic models (CanESM5, BCC-CSM2-MR, and MRI-ESM2-0) play the vital role in the simulated results, are presented in Fig. 9. As shown, BCC-CSM2-MR has the highest impact (about 48.4%) on the estimated temperature in the downscaling process. Furthermore, CanESM5 and MRI-ESM2-0 achieved 22.9% and 28.8% for the SA percentage, respectively. Therefore, daily temperature predictions are most sensitive to BCC-CSM2-MR outputs.

3.4 Pros and cons of MGGP-based downscaling method

One of the advantages of applying MGGP as a downscaling model is that the structure and its components (functions, parameters, and coefficients) of the predictand-predictor relationship can be determined by MGGP. In other words, MGGP can develop prediction models without shape limitation (Zakwan and Niazkar 2021, 2022). Furthermore, MGGP provides explicit equations that can be used in other relevant applications on climate change. In contrast, ANN will work as a black box model, which does not give an explicit relation for downscaling purposes. Moreover, by playing with the most important controlling parameters of MGGP (the maximum genes allowed in each individual and the tree depth), it can develop different equations with various range of complexity and accuracy. Therefore, the user of MGGP model can tune MGGP controlling parameters to address the trade-off and consequently achieve an estimation model with desirable precision and complexity. In

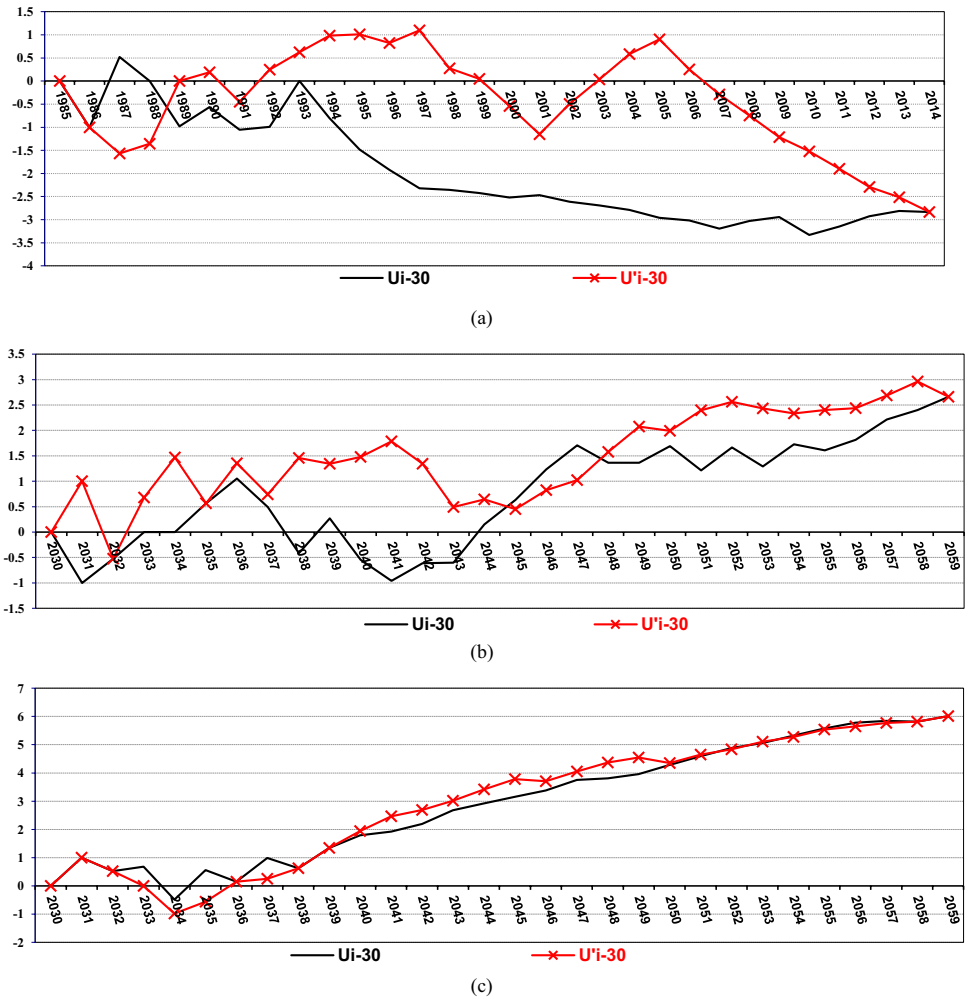

Fig. 7 Changes of $U(t_i)$ and $U'(t_i)$ components for average annual temperatures of **a** observed data, **b** SSP1 scenario, and **c** SSP5 scenario

Table 4 Results of the MK test and Sen's slope estimator at 95% and 99% confidence levels for monthly data

Month	Observed data		SSP1 scenario		SSP5 scenario	
	Z	*Q*	*Z*	*Q*	*Z*	*Q*
January	−1.11	−0.041	−1.96*	0.027	3.85**	0.075
February	0.39	0.014	2.39*	0.033	4.07**	0.068
March	1.07	0.046	0.96	0.029	3.75**	0.072
April	−0.62	−0.021	2.36*	0.057	4.5**	0.123
May	−0.89	−0.031	3**	0.045	4.78**	0.078
June	−1.14	−0.031	0.21	0.003	2.75**	0.017
July	−1.8*	−0.046	0.79	0.007	1.11	0.006
August	−3.53**	−0.067	0.14	0.001	4.42**	0.026
September	−1.94*	−0.054	−0.43	−0.003	3.07**	0.038
October	−2.6**	−0.05	1.21	0.018	2.32**	0.055
November	−2.12*	−0.08	−0.57	−0.008	3.46**	0.097
December	−1.07	−0.033	−0.07	−0.002	4.50**	0.092

*Existence of trends at the level of 95%

**Existence of trends at the level of 99%

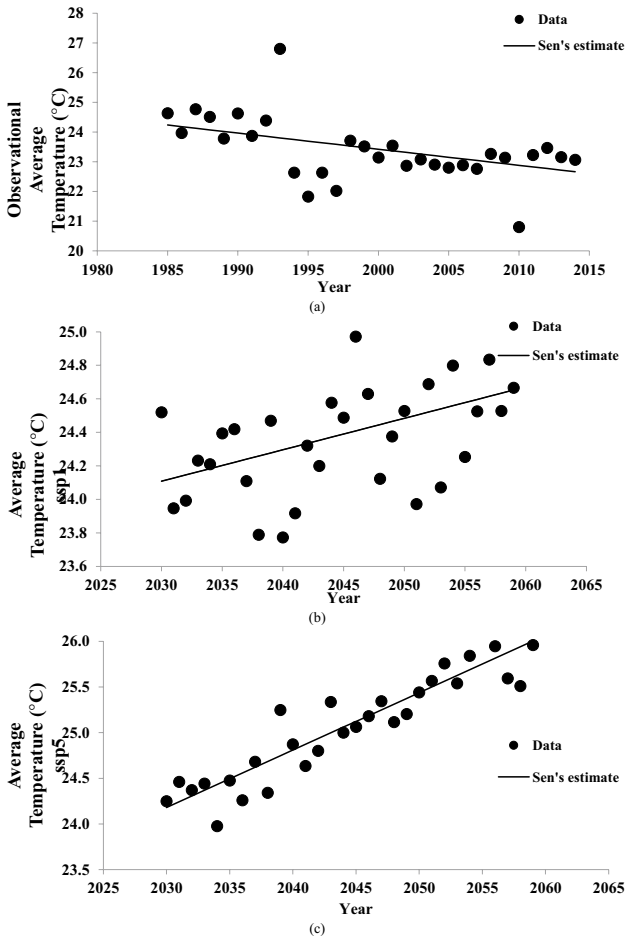

Fig. 8 Sen's slope diagrams for the average temperature of **a** observed data, **b** SSP1 scenario, and **c** SSP5 scenario

this regard, poor selections of the controlling parameters of MGGP may result in unsolicited estimations. Thus, the controlling parameters of MGGP are required to be set either in accordance with previous studies or by conducting trial-and-error examinations. In addition to the controlling parameters of MGGP, a careful attention needs to be paid when running it for developing an ML-based downscaling model. Since each run of MGGP can inevitably give a unique equation, running for a considerable number of times (e.g., 50 times) may be required to ensure about the applicability of the MGGP results. Although MGGP was found to be not only a reliable but also an accurate downscaling model, further investigations on different study areas may be required to draw a conclusion on how MGGP performs as an ML-based downscaling model. Finally, developing ensemble downscaling models including MGGP-based models may also be one of the future trends for continuing research in light of developing downscaling methods with higher accuracy.

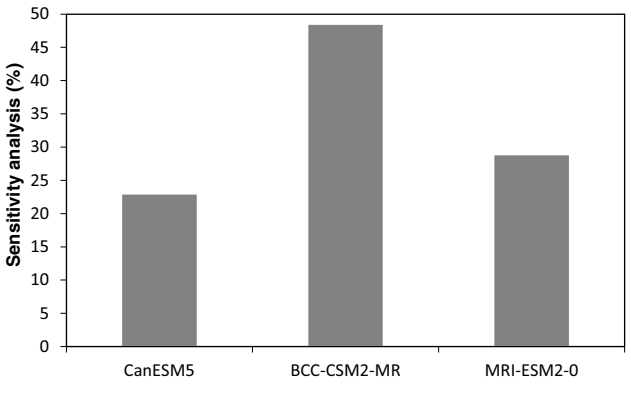

Fig. 9 Results of the sensitivity analysis of MGGP-based statistical downscaling model

4 Conclusions

This study utilized MGGP as a statistical downscaling method for developing predictand-predictor relationships for the first time. The daily temperature values observed from 1985 to 2015 at Dogonbadan station, Kohgiluyeh and Boyer-Ahmad Province, Iran, were used not only to training but also to test ML-based downscaling methods. The outputs of three climatic models (CanESM5, BCC-CSM2-MR, and MRI-ESM2-0) were downscaled using the sixth report. Unlike ANN, MGGP can develop an explicit equation for downscaling GCM outputs. The comparative analysis conducted between the estimated and observed daily temperature for the historical period indicates (1) both ML-based downscaling models performed acceptably accurate and (2) MGGP slightly improved the estimations of the test data achieved by ANN based on three metrics. MGGP can be used as a tool for conducting a sensitivity analysis. The sensitivity analysis showed that the MGGP-based downscaling model is sensitive to CanESM5, BCC-CSM2-MR, and MRI-ESM2-0 by 22.9, 48.4, and 28.8%, respectively. Furthermore, the ML-based downscaling models were exploited to forecast daily temperature during 2030–2060 for two scenarios (SPP1 and SPP5). Generally, the Mann–Kendall's test and Sen's slope estimator for the two scenarios indicate an increasing trend of the observed and estimated temperatures in the most of future months. Furthermore, the future predictions revealed that the maximum daily temperature will reduce, whereas the minimum daily temperature will increase, even up to 10 °C for a few years, between 2030 and 2060. A few advantages and drawbacks of MGGP as a statistical downscaling model were presented and discussed, while further assessment of MGGP applications for this purpose were found to be required before drawing a wide-ranging conclusion.

Acknowledgements The authors would like to thank IPCC, the international community, and local data providers. Indeed, this study could not be done without their support in providing us with the data required.

Author contribution MN: conceptualization; investigation; methodology; formal analysis; validation; writing—original draft; review and editing; resources; journal format preparation. MG: conceptualization; investigation; supervision; resources; data curation; writing—review and editing; project administration. AF: conceptualization; methodology; data curation; formal analysis; writing—original draft; writing—review and editing; validation. MJA: formal analysis. All authors read and approved the final manuscript.

Data availability Data are however available from the authors upon a reasonable request.

Code availability Not applicable.

Declarations

Ethics approval Not applicable.

Consent to participate Not applicable.

Consent for publication Not applicable.

Competing interests The authors declare no competing interests.

References

Ahmed K, Shahid S, Haroon SB, Xiao-jun W (2015) Multilayer perceptron neural network for downscaling rainfall in arid region: a case study of Baluchistan, Pakistan. J Earth Syst Sci 124:1325–1341

Akurut M, Willems P, Niwagaba CB (2014) Potential impacts of climate change on precipitation over Lake ictoria, East Africa, in the 21st Century. Water 2114(6):2634–2659

Almazroui M, Saeed S, Saeed F, Islam MN, Ismail M (2020) Projections of precipitation and temperature over the South Asian countries in CMIP6. Earth Syst Environ 4(2):297–320

Beecham S, Rashid M, Chowdhury RK (2014) Statistical downscaling of multi-site daily rainfall in a South Australian catchment using a Generalized Linear Model. Int J Climatol 34:3654–3670

Chen H, Xu CY, Guo S (2012) Comparison and evaluation of multiple GCMs, statistical downscaling and hydrological models in the study of climate change impacts on runoff. J Hydrol 434:36–45

Coulibaly P (2004) Downscaling daily extreme temperatures with genetic programming. Geophys Res Lett 31:L16203

Duan K, Mei Y (2014) A comparison study of three statistical downscaling methods and their model-averaging ensemble for precipitation downscaling in China. Theoret Appl Climatol 116(3–4):707–719

Estoque RC, Ooba M, Togawa T, Hijioka Y (2020) Projected land-use changes pathways describing world futures in the 21st century. Glob Environ Chang 42:169–180

Eyring VS, Bony GA, Meehl CA et al (2016) Overview of the Coupled Model Intercomparison Project Phase 6 (CMIP6) experimental design and organization. Geosci Model Dev 9:1937–1958. https://doi.org/10.5194/gmd-9-1937-2016

Ghosh S, Mujumdar P (2008) Statistical downscaling of GCM simulations to streamflow using relevance vector machine. Adv Water Resour 31:132–146

Gidden MJ, Riahi K, Smith SJ, Fujimori S, Luderer G, Kriegler E, Takahashi K (2019a) Global emissions pathways under different socioeconomic scenarios for use in CMIP6: a dataset of harmonized emissions trajectories through the end of the century. Geoscientific Model Development. https://doi.org/10.5194/gmd-12-1443-2019

Gidden M, Riahi K, Smith S, Fujimori S, Luderer G, Kriegler E, Calvin K (2019) Global emissions pathways under different socioeconomic scenarios for use in CMIP6: a dataset of harmonized emissions trajectories through the end of the century. Geosci Model Dev Discuss 12:1443–1475

Goly A, Teegavarapu RSV, Mondal A (2014) Development and evaluation of statistical downscaling models for monthly precipitation. Earth Interact 18:1–28

Goodarzi MR, Fatehifar A, Moradi A (2020) Predicting future flood frequency under climate change using Copula function. Water Environ J 34:710–727

Goodarzi MR, Mohtar RH, Piryaei R, Fatehifar A, Niazkar M (2022) Urban WEF nexus: an approach for the use of internal resources under climate change. Hydrology 9(10):176. https://doi.org/10.3390/hydrology9100176

Hao Z, Aghakouchak A, Phillips TJ (2013) Changes in concurrent monthly precipitation and temperature extremes. Environ Res Lett 8:1–7

Hashmi MZ, Shamseldin AY, Melville BW (2011) Statistical downscaling of watershed precipitation using Gene Expression Programming (GEP). Environ Modell Software 26:1639–1646

Hirca T, Eryılmaz Türkkan G, Niazkar M (2022) Applications of innovative polygonal trend analyses to precipitation series of Eastern Black Sea Basin Turkey. Theoretical Appl Climatol 147(1):651–667. https://doi.org/10.1007/s00704-021-03837-0

IPCC (2018) GlobalWarming of 1.58C.V.Masson-Delmotteetal.,Eds., Cambridge University Press, 630 pp., https://www.ipcc.ch/site/assets/uploads/sites/2/2019/06/SR15_Full_Report_Low_Res.pdf

Kumar YP, Maheswaran R, Agarwal A, Sivakumar B (2021) Intercomparison of downscaling methods for daily precipitation with emphasis on wavelet-based hybrid models. J Hydrol 599:126373

Mendez M, Maathuis B, Hein-Griggs D, Alvarado-Gamboa LF (2020) Performance evaluation of bias correction methods for climate change monthly precipitation projections over Costa Rica. Water 12(2):482

Niazkar M (2020) Assessment of artificial intelligence models for calculating optimum properties of lined channels. J Hydroinf 22(5):1410–1423. https://doi.org/10.2166/hydro.2020.050

Niazkar M (2021) (2021) Optimum design of straight circular channels incorporating constant and variable roughness scenarios: assessment of machine learning models. Math Prob Eng 2021:1–21. https://doi.org/10.1155/2021/9984934 (Article ID 9984934)

Niazkar M (2021) Zakwan M (2021) Assessment of artificial intelligence models for developing single-value and loop rating curves. Complexity 2021:1–21. https://doi.org/10.1155/2021/6627011 (Article ID 6627011)

Nourani V, Razzaghzadeh Z, Baghanam AH, Molajou A (2019) ANN-based statistical downscaling of climatic parameters using decision tree predictor screening method. Theoret Appl Climatol 137(3):1729–1746

Okkan U, Inan G (2015) Statistical downscaling of monthly reservoir inflows for Kemer watershed in Turkey: use of machine learning methods, multiple GCMs and emission scenarios. Int J Climatol 35(11):3274–3295

Partal T, Kahya E (2006) Trend analysis in Turkish precipitation data. Hydrol Process: Int J 20(9):2011–2026

Riahi K, Van Vuuren DP, Kriegler E, Edmonds J, O'neill BC, Fujimori S, Bauer N, Calvin K, Dellink R, Fricko O, Lutz W (2017) The shared socioeconomic pathways and their energy, land use, and greenhouse gas emissions implications: an overview. Global Environ Change 42:153–168

Sachindra DA, Huang F, Barton AF, Perera BJC (2013) Least square support vector and multi-linear regression for statistically downscaling general circulation model outputs to catchment streamflows. Int J Climatol 33:1087–1106

Sachindra DA, Huang F, Barton AF, Perera BJC (2014) Multi-model ensemble approach for statistically downscaling general circulation model outputs to precipitation. Q J Roy Meteor Soc 140:1161–1178

Sachindra DA, Ng AWM, Muthukumaran S, Perera BJC (2016) Impact of climate change on urban heat island effect and extreme temperatures: a case-study. Q J Roy Meteor Soc 142:172–186

Sachindra DA, Kanae S (2019) Machine learning for downscaling: the use of parallel multiple populations in genetic programming. Stoch Env Res Risk Assess 33(8):1497–1533

Sachindra DA, Ahmed K, Rashid MM, Sehgal V, Shahid S, Perera BJC (2019) Pros and cons of using wavelets in conjunction with genetic programming and generalised linear models in statistical downscaling of precipitation. Theoret Appl Climatol 138(1):617–638

Sachindra DA, Ahmed K, Rashid MM, Shahid S, Perera BJC (2018a) Statistical downscaling of precipitation using machine learning techniques. Atmos Res 212:240–258

Sachindra DA, Ahmed K, Shahid S, Perera BJC (2018b) Cautionary note on the use of genetic programming in statistical downscaling. Int J Climatol 38(8):3449–3465

Salmi T, Maatta A, Anttila P, Ruoho-Airola T, Amnell T (2002) Detecting trends of annual values of atmospheric pollutants by the Mann-Kendall test and Sen's slope estimates—the excel template application MAKESENS. Ilmanlaadun julkaisuja Publikationer om luftkvalitet Publications on air quality, No. 31

Serrano A, Mateos VL, Garcia JA (1999) Trend analysis of monthly precipitation over the iberian peninsula for the period 1921–1995. Phys Chem Earth Part B 24(1):85–90. https://doi.org/10.1016/S1464-1909(98)00016-1

Swart Neil C, Cole Jason NS, Kharin Viatcheslav V et al (2019) The Canadian earth system model version 5 (CanESM5. 0.3). Geosci Model Dev 12(11):4823–4873

Tripathi S, Srinivas VV, Nanjundiah RS (2006) Downscaling of precipitation for climate change scenarios: a support vector machine approach. J Hydrol 330(3–4):621–640

Vu MT, Aribarg T, Supratid S, Raghavan SV, Liong SY (2016) Statistical downscaling rainfall using artificial neural network: significantly wetter Bangkok? Theoret Appl Climatol 126(3–4):453–467

Wu T, Lu Y, Fang Y et al (2019) The Beijing Climate Center climate system model (BCC-CSM): The main progress from CMIP5 to CMIP6. Geosci Model Dev 12:1573–1600

Wu Tongwen, Chu Min, Dong Min et al (2018). BCC BCC-CSM2MR model output prepared for CMIP6 CMIP piControl. Version YYYYMMDD[1]. Earth System Grid Federation. https://doi.org/10.22033/ESGF/CMIP6.3016

Yue Y, Yan D, Yue Q, Ji G, Wang Z (2021) Future changes in precipitation and temperature over the Yangtze River Basin in China based on CMIP6 GCMs. Atmos Res 264:105828. https://www.sciencedirect.com/science/article/pii/S0169809521003847

Yukimoto S, Kawai H, Koshiro T, Oshima N, Yoshida K, Urakawa S et al (2019) The Meteorological Research Institute Earth System Model version 2.0, MRI-ESM2. 0: description and basic evaluation of the physical component. J Meteorol Soc Jpn Ser II. https://doi.org/10.2151/jmsj.2019-051

Zakwan M, Niazkar M (2022) Innovative triangular trend analysis of monthly precipitation at Shiraz Station, Iran. In: Current Directions in Water ScarcityResearch, vol. 7. Elsevier, New York, pp589-598

Zakwan M, Niazkar M (2021) A comparative analysis of data-driven empirical and artificial intelligence models for estimating infiltration rates. Complexity 2021:1–13. https://doi.org/10.1155/2021/9945218 (Article ID 9945218)

Zerenner T, Venema V, Friederichs P, Simmer C (2018) Downscaling daily station precipitation amounts using deterministic and stochastic regression models generated by multi-objective genetic programming. In: EGU General Assembly Conference Abstracts, p. 15007. https://ui.adsabs.harvard.edu/abs/2018EGUGA..2015007Z/abstract

Zerenner T, Venema V, Friederichs P, Simmer C (2021) Multi-objective downscaling of precipitation time series by genetic programming. Int J Climatol 41(14):6162–6182. https://doi.org/10.1002/joc.7172